



HAL
open science

New method to quantify hydrophobicity of non-enveloped virions in aqueous media by capillary zone electrophoresis

Guillaume Bastin, Christophe Gantzer, Guillaume Sautrey

► **To cite this version:**

Guillaume Bastin, Christophe Gantzer, Guillaume Sautrey. New method to quantify hydrophobicity of non-enveloped virions in aqueous media by capillary zone electrophoresis. *Virology*, 2022, 568, pp.23-30. 10.1016/j.virol.2022.01.004 . hal-03553130

HAL Id: hal-03553130

<https://hal.univ-lorraine.fr/hal-03553130>

Submitted on 22 Jul 2024

HAL is a multi-disciplinary open access archive for the deposit and dissemination of scientific research documents, whether they are published or not. The documents may come from teaching and research institutions in France or abroad, or from public or private research centers.

L'archive ouverte pluridisciplinaire **HAL**, est destinée au dépôt et à la diffusion de documents scientifiques de niveau recherche, publiés ou non, émanant des établissements d'enseignement et de recherche français ou étrangers, des laboratoires publics ou privés.



Distributed under a Creative Commons Attribution - NonCommercial 4.0 International License

1 **Title:**

2 **New Method to Quantify Hydrophobicity of Non-enveloped Virions**
3 **in Aqueous Media by Capillary Zone Electrophoresis**

4
5 **Authors:**

6 Guillaume Bastin, Christophe Gantzer, Guillaume Sautrey*

7
8 **Affiliation:**

9 LCPME UMR 7564, Université de Lorraine – CNRS, 405 rue de Vandoeuvre 54600
10 Villers-lès-Nancy, France.

11

12 * **Corresponding author:**

13 Dr. Guillaume Sautrey,

14 Tel: +33 3 72 74 74 12.

15 E-mail address: guillaume.sautrey@univ-lorraine.fr

16

17 **Keywords:**

18 Bacteriophage; virion; hydrophobicity; non-enveloped virus; pH; capillary zone
19 electrophoresis; SDS; aqueous media.

20

21 **Abstract**

22 The hydrophobicity of virions is a major physicochemical parameter regulating their
23 dissemination in humans and the environment. But knowledge about potential factors
24 modulating virion hydrophobicity is limited due to the lack of suitable quantifying
25 methods. It has been recently shown that sodium dodecyl-sulfate (SDS) labels capsid
26 hydrophobic domains in capillary zone electrophoresis of non-enveloped virions,
27 altering their electrophoretic mobility (μ) in proportion to their hydrophobicity. This
28 was exploited here to quantify the hydrophobicity of GA, Q β and MS2 phages as a
29 function of pH. By subtracting the native from the SDS-modified μ of phages,
30 measured in the absence and presence of SDS, respectively, we defined a
31 "hydrophobic index" increasing with virion hydrophobicity. Using this approach, we
32 found that the virion hydrophobicity changes at a virion-specific pivotal pH. This
33 procedure may be applied under various physicochemical conditions and to diverse
34 non-enveloped virus families of significance to human health and the environment.

35

36

37

38 **1. Introduction**

39 The replication cycle of viruses includes an extracellular period during which viral
40 particles, called virions, may reach the environment to reside for weeks/months. At
41 this stage, the physicochemical surface properties of virions largely modulate their
42 adhesion to diverse surfaces (Gerba, 1984). Notably, change in the electrical charge
43 and/or hydrophobicity of virions in response to fluctuations in the environment (e.g.
44 pH, temperature, or ionic strength) inevitably impact the fate of viruses. Therefore,
45 understanding these physicochemical dynamics is important to predict transmission
46 routes of viruses and to better control their dissemination as recently emphasized
47 with the COVID-19 outbreak (Joonaki et al., 2020).

48 Both charge-charge and hydrophobic interactions cooperate by acting in a
49 'supralinear' way (Stefan and Le Novère, 2013) and therefore must be considered
50 together when studying virion adhesion processes (Gerba, 1984). The overall electric
51 charge of virions can be assessed by considering their isoelectric point (pHi) (Michen
52 and Graule, 2010), i.e. the pH value at which the virion charge reverses. But the
53 interpretation of pHi values may be unreliable in describing the ionization degree of
54 virions beyond this equilibrium pH (Dika et al., 2015; Heffron and Mayer, 2021;
55 Langlet et al., 2008a). The electrophoretic mobility (μ) of virions can provide
56 quantitative information about their surface charge density outside their pHi (Heffron
57 and Mayer, 2021). It is known that the electric charge of virions changes non-linearly
58 as a function of pH (Armanious et al., 2016; Langlet et al., 2008a; Shi and Tarabara,
59 2018) and ionic strength (Dika et al., 2013b; Langlet et al., 2008a). The
60 hydrophobicity of virions also varies between viruses (Armanious et al., 2016; Dika et
61 al., 2013b; Shi and Tarabara, 2018), but the dynamics of virion hydrophobicity and
62 potential physicochemical factors affecting it remain to be characterized. The pH of

63 the virion environment may be such a factor, as pH variations can induce structural
64 rearrangements in the proteinaceous capsid (Roshal et al., 2019; Song et al., 2020),
65 modifying the surface exposure of hydrophobic amino acid residues that should have
66 an impact on virion hydrophobicity. The protonation/deprotonation equilibria of
67 alkaline/acidic amino acid residues in the capsid are also expected to impact the
68 hydrophobic/hydrophilic balance of virions (Dika et al., 2013b). Therefore, like
69 electrical charge, the hydrophobicity of virions should be considered dynamically in
70 response to pH variation.

71 The electrophoretic mobility μ of all electrically charged molecular species
72 depends on their size-to-charge ratio. This is the separative principle of capillary zone
73 electrophoresis (CZE) (Shintani, 1997). But for macromolecular assemblies like
74 viruses, the charged surface leads to the formation of an electric double layer (EDL)
75 and thus to a zeta potential (ζ) (Hunter, 1981a, 1981b). Therefore the molecular
76 electrokinetic model of CZE becomes irrelevant with viruses (Kenndler, 2001). To
77 describe the electromigration of virions in CZE, several electrokinetic theories can be
78 applied depending on a ratio of the virion's radius R to the reciprocal of the Debye
79 parameter K (i.e. the thickness of the EDL), the latter being influenced by the ionic
80 strength I of the medium ($K \sim \sqrt{I}$). For moderate ionic strengths (i.e. 10-100 mM), the
81 thickness of the EDL formed around a virion is much smaller than its radius.
82 According to the Smoluchowsky electrokinetic model, the μ value of a virion becomes
83 thus proportional to its ζ potential, itself being proportional to the virion's charge
84 density and to the K value (Kenndler, 2001). Interestingly, it has been recently
85 reported that adding an anionic amphiphilic compound, sodium dodecyl-sulfate
86 (SDS), to the background electrolyte (BGE) used for CZE analyses resulted in a μ
87 shift for MS2 and Q β phages in comparison with similar SDS-free analyses (Sautrey

88 et al., 2018). This effect has been shown to be related to non-polar interactions of the
89 lipophilic tail of SDS molecules with capsid hydrophobic domains, exposing in their
90 stead the negatively charged hydrophilic head of SDS molecules, thereby increasing
91 the negative charge density of virions. One can thus hypothesize that the more SDS
92 changes the μ value of virions the more capsids have hydrophobic domains. Based
93 on this line of thought, the SDS-induced shifting of μ values in CZE analyses of
94 virions can be exploited to quantify virion hydrophobicity in aqueous media.

95 MS2, GA and Q β are bacteriophages belonging to the *Leviviridae*. The virions
96 consist of a positive single stranded RNA enclosed in an icosahedral capsid (27 nm
97 diameter) made from 178 copies of a single coat protein (Golmohammadi et al.,
98 1996, 1993; Tars et al., 1997). The capsids also include one copy of a maturation
99 protein bound to the RNA genome and that is essential for the virions to be infectious
100 (Cui et al., 2017; Dent et al., 2013). These bacteriophages infect *Escherichia coli* in
101 the human or animal intestine; they are therefore sometimes released in feces and
102 follow the fecal oral route to infect new hosts. Being structurally similar to most
103 enteric viruses pathogenic to humans and following similar environmental routes,
104 MS2, GA and Q β are often used to predict the dissemination of waterborne enteric
105 viruses in the environment and their accumulation in food products (Farkas et al.,
106 2020; Hodgson et al., 2017). The persistence of phages *in vivo* is equally important in
107 the context of their use in therapy situations (Serwer et al., 2021). The rate of their
108 removal from blood by the reticuloendothelial system (Merril et al., 1996) involves the
109 physicochemical adhesion of virions to the surface of cells specialized in blood
110 clearing. For these purposes, MS2, GA and Q β phages have been used as models
111 for studying virion hydrophobicity (Armanious et al., 2016; Boudaud et al., 2012; Dika
112 et al., 2013b; Langlet et al., 2008a). However, virion hydrophobicity was considered

113 as a constant parameter, and its dynamics in response to environmental changes,
114 notably pH variations, remain to be evidenced in order to provide a comprehensive
115 prediction of the dissemination of viruses in aqueous media.

116 The strategy here was thus to measure the SDS-induced shift in the μ value of
117 MS2, GA and Q β phages as a function of pH from 4 to 11 by CZE analyses
118 performed in the absence and presence of 10 mM SDS. These shifts were
119 determined by subtracting the native μ value ($\mu_{native}^{phage, pH}$) from the corresponding SDS-
120 modified μ ($\mu_{SDS-modified}^{phage, pH}$) to quantify the hydrophobicity of virions by means of a
121 'hydrophobic index' (symbolized H_{pH}^{phage}). Importantly, all phosphate buffers used as
122 BGE were prepared to ensure 10 mM ionic strength by adjusting the phosphate
123 concentration according to the desired pH value, otherwise (i) changes in the Debye
124 parameter K of the virions depending on the ionic strength of the medium are likely to
125 interfere with the measurements (Kenndler, 2001; Langlet et al., 2008a), and (ii)
126 phage aggregation often occurred beyond 100 mM ionic strength (Langlet et al.,
127 2008a) may also interfere in measurements by preventing SDS binding to the virions
128 buried within aggregates. Following this procedure, we found that the hydrophobicity
129 of MS2, GA and Q β phages changes suddenly at a phage-specific pivotal pH. This is
130 possibly also true for other non-enveloped virus families and other physicochemical
131 factors.

132

133 **2. Materials and methods**

134 **2.1. Chemical and reagents**

135 Phosphoric acid $\geq 85\%$ (14.6 M), sodium dodecyl-sulfate (SDS), dimethyl
136 sulfoxide (DMSO) and other reagents in analytical grade were from Sigma Aldrich
137 (Saint Louis, USA). Ultrapure water was obtained in a Purelab Ultra MKII system
138 from Elga (Le Plessis Robinson, France).

139

140 **2.2. Production and purification of bacteriophages**

141 MS2, GA and Q β were all produced, purified and enumerated using described
142 protocols (Bastin et al., 2020). The final concentrations of purified phage suspensions
143 in 1 mM PBS (13.7 mM NaCl, 0.27 mM KCl, 1.0 mM Na₂HPO₄, 0.18 mM KH₂PO₄, pH
144 7.4) were 4×10^{13} PFU/mL for MS2, 1×10^{13} PFU/mL for Q β , and 5×10^{12} PFU/mL for
145 GA. The stock suspensions were stored at 4°C and away from light until use.

146

147 **2.3. Capillary zone electrophoresis (CZE)**

148 CZE experiments were performed on a PA 800 *Plus* Pharmaceutical Analysis
149 System apparatus (SCIEX) equipped with a diode array UV/vis detector operating
150 between 200 and 300 nm and located at the outlet side of the capillary. Data
151 acquisition and processing were performed using the 32 Karat software supplied by
152 SCIEX, and electropherograms at 214 nm were analyzed. A fused-silica capillary 75
153 μ m internal diameter (Polymicro Technologies, Caudebec les Elboeuf, France), 30
154 cm total length (from the inlet to the outlet) and 20 cm effective length (from the inlet
155 to the UV detection window) was employed. Capillary temperature was controlled by
156 coolant at 25.0 °C. All solutions were filtered before use with a 0.45 μ m pore size
157 regenerated cellulose filter (Alltech, Templeuve, France). Analyses were

158 accomplished using phosphate buffers as background electrolytes (BGEs),
159 supplemented or not with 10 mM SDS. The BGEs were prepared by diluting
160 appropriate volume of 0.85% H₃PO₄ aqueous solution (146 mM) to reach the
161 required concentration for a final 10 mM ionic strength depending on the desired pH
162 (please, read Appendix A for details), and eventually by dissolving SDS powder in
163 ultrapure water. The pH was adjusted with 1 M NaOH, and ultrapure water was
164 added up to final volume.

165 A neutral marker was prepared by diluting pure DMSO (0.005% v/v) in ultrapure
166 water or in 10 mM SDS aqueous solution in order to measure the mobility μ_{EOF} of the
167 electroosmotic flow (EOF) for each analysis. The ionic strength of stock phage
168 suspensions was reduced by one-tenth dilution in ultrapure water or in 10 mM SDS
169 aqueous solution prior to analysis in order to avoid variable stacking effects within
170 each phage sample at the beginning of CZE runs. The final concentrations of viral
171 samples were 4×10^{12} PFU/mL for MS2, 1×10^{12} PFU/mL for Q β and, 5×10^{11} PFU/mL
172 for GA. For CZE analyses of the three phages together (Fig. 1a and 2a), 5 μ L of 10-
173 fold diluted phage suspensions were mixed directly into a vial prior to injection.

174 The analytical method consisted of successive rinses using 1 M NaOH (2 min),
175 ultrapure water (2 min) and BGE (2 min). Then, the DMSO and viral samples were
176 successively injected at the inlet side of the capillary in the hydrodynamic forward
177 mode under 0.5 psi pressure (3 s for DMSO solution then 5 s for viral suspension),
178 both sides of the capillary were immersed in BGE, and 10 kV voltage was applied
179 (normal polarity). The EOF is then oriented from the anodic inlet side to the detection
180 window near the cathodic outlet side. The virions, being negatively charged, are
181 attracted to the anode (i.e. by their electrophoretic mobility μ) while being pulled
182 towards the cathode by the EOF oriented in the opposite direction. Thus, virions

183 migrate more slowly than DMSO, and the more their negative charge density, the
184 longer is their migration time. All analyses were performed at least in triplicate in
185 order to evaluate the residual standard deviation (RSD) for each measurement.

186

187 **2.4. Mobility and hydrophobic index calculation**

188 In CZE performed in normal polarity, each species injected at the inlet of the
189 BGE-filled capillary are mobilized toward the detection window under the influence of
190 a high voltage applied between both sides of the capillary. The migration velocity of
191 the analytes is governed by their apparent mobility (μ_{app}) which can be determined
192 from measurement of their migration time according to the following relation
193 (Shintani, 1997):

$$194 \mu_{app} = \frac{L \times l}{\Delta V \times t_m} \quad (1)$$

195 where μ_{app} is the apparent mobility of the considered analyte, L is the capillary total
196 length expressed in meter, l is the capillary effective length from the inlet to the
197 detection window (meters), ΔV is the applied electrical potential expressed in volt and
198 t_m is the migration time of the analyte expressed in seconds.

199 The apparent mobility of each analyte is so called because it is the outcome of
200 two intrinsic mobilities, namely the electroosmotic mobility (μ_{eof}) and the
201 electrophoretic mobility (μ) as shown in the following relation:

$$202 \mu_{app} = \mu + \mu_{eof} \quad (2)$$

203 where μ_{eof} is a driving force both for ionic and neutral species, which depends on the
204 BGE composition, while μ is a specific feature of electrically charged analytes
205 depicting their electrostatic attraction to either of the two electrodes located at the
206 capillary extremities.

207 With neutral species like DMSO, where there are no cathodic or anodic
 208 attractions, μ is null. Such neutral species are therefore mobilized only according to
 209 the EOF, enabling determination of the μ_{eof} value from the relation (3) by combining
 210 the relations (1) and (2):

$$211 \mu_{app}^{DMSO} = \mu_{eof} = \frac{L \times I}{\Delta V \times t_m^{DMSO}} \quad (3)$$

212 where μ_{app}^{DMSO} is the apparent mobility of DMSO and t_m^{DMSO} is its migration time.

213 From a single run performed by co-injecting a DMSO sample as an EOF marker
 214 and a phage sample as an electrically charged entity, we applied relation (3) with the
 215 DMSO migration time to determine the μ_{eof} value while relation (1) was applied with
 216 the phage migration time to determine the μ_{app} of virions. Finally, according to
 217 relation (2), both relations (1) and (3) were combined to determine the μ of virions:

$$218 \mu^{virion} = \mu_{app}^{virion} - \mu_{app}^{DMSO} = \frac{L \times I}{\Delta V \times t_m^{virion}} - \frac{L \times I}{\Delta V \times t_m^{DMSO}} = \frac{L \times I}{\Delta V} \left(\frac{1}{t_m^{virion}} - \frac{1}{t_m^{DMSO}} \right) \quad (4)$$

219 where μ_{app}^{virion} and μ^{virion} are, respectively, the apparent and electrophoretic mobilities
 220 of a phage while t_m^{virion} is its migration time.

221 By applying relation (4), the native μ value of a phage at a given pH ($\mu_{native}^{phage, pH}$)
 222 was determined from CZE analysis without SDS, while the corresponding SDS-
 223 modified μ value ($\mu_{SDS-modified}^{phage, pH}$) was determined similarly from CZE analysis in the
 224 presence of 10 mM SDS. The hydrophobic index of phages as a function of pH
 225 (H_{pH}^{phage}) was calculated by subtracting the $\mu_{native}^{phage, pH}$ values from the $\mu_{SDS-modified}^{phage, pH}$
 226 values, both expressed in terms of dimensionless quantities by normalizing mobilities
 227 with physical constants to undo their units (Radko et al., 2000):

$$228 H_{pH}^{phage} = \left(\mu_{SDS-modified}^{phage, pH} - \mu_{native}^{phage, pH} \right) \times \frac{3\eta e}{2\epsilon kT} \quad (5)$$

229 where ϵ and η are respectively the permittivity and the viscosity of the BGE (taken
230 as those of water that are 6.94×10^{-10} F.m⁻¹ and 8.90×10^{-4} Pa.s, respectively), k is the
231 Boltzmann constant (1.38×10^{-23} m².Kg.s⁻².K⁻¹), T is the absolute temperature (298 K)
232 and e is the electron charge (1.60×10^{-19} C).

233

234 **2.5. Prediction of protein hydrophobicity from primary sequence analysis**

235 Online protscale software from the expasy platform was used. The software can
236 be found via the following internet link as it was on January 01, 2022:
237 <https://web.expasy.org/protscale/>

238 For prediction of hydrophobicity, a seven amino acids smoothing average window
239 was used for analysis by using the algorithm “Kyte and Doolittle”. Hydrophobic amino
240 acid corresponding score can be found at the following internet link:
241 <https://web.expasy.org/protscale/pscale/Hphob.Doolittle.html>

242 The sequences for capsid protein of GA, Q β and MS2 phages were all from the
243 UniProtKB data base with the following reference numbers: GA: P07234
244 (CAPSD_BPGA); MS2: P03612 (CAPSD_BPMS2); Q β : P03615 (CAPSD_BPQBE).

245 **3. Results and discussion**

246 **3.1. CZE assays with SDS-free BGEs: native electrophoretic mobilities**

247 To illustrate the accuracy achieved by electrophoretic mobility measurement in
248 CZE, a sample containing the three phages MS2, Q β and GA was analyzed at pH 7
249 by co-injection with an aqueous solution of DMSO (used as the EOF marker). Each
250 phage was detected as a single narrow peak, indicating no alteration of virions by the
251 process of electrophoresis (Sautrey et al., 2018), and at a repeatable migration time
252 of 1.75, 2.26 and 3.42 min for GA, Q β and MS2, respectively (Fig. 1a). Peaks
253 identification was made by individually analyzing each phage, which resulted in the
254 same migration times as when pooled. All three phages were slower than DMSO at
255 pH 7 (Fig. 1a), indicating a negative $\mu_{native}^{phage, 7}$ that is opposed to the EOF and signifies
256 that virions are negatively charged (see Section 2.3). This is consistent with a
257 previous study (Michen and Graule, 2010). Focusing on individual phages, GA was
258 faster than Q β , which is much faster than MS2 (Fig. 1a). This indicates $\mu_{native}^{MS2, 7} \ll$
259 $\mu_{native}^{Q\beta, 7} < \mu_{native}^{GA, 7}$ (see Section 2.4 for details of data processing), suggesting the
260 negative charge density order MS2>>Q β >GA. This order is inconsistent with previous
261 reports in which the negative charge density of MS2, Q β and GA were similar at pH 7
262 (Dika et al., 2013b; Langlet et al., 2008a; Shirasaki et al., 2009). The difference may
263 be due to disparities in the protocols in preparing the viral samples prior to
264 electrophoretic mobility measurements (e.g. purification methods may impact the
265 virion surface properties) (Dika et al., 2013a; Langlet et al., 2008a; Shi and Tarabara,
266 2018).

267 Each phage was then individually analyzed by co-injection with DMSO and using
268 SDS-free BGEs at a pH range from 4 to 11 (all at 10 mM ionic strength). Importantly,
269 the electric current intensities measured in the capillary during CZE analysis were

270 similar (Fig. S1) indicating equivalent ionic strengths for all BGEs (Kuhn and
271 Hoffstetter-Kuhn, 1993). From these experiments, the native electrophoretic mobility
272 $\mu_{native}^{phage, pH}$ of MS2, Q β and GA phages was plotted against pH (Fig. 1b). However, on
273 both sides of the pH range examined, the electrophoretic mobility measurement
274 became unreliable for all three phages (residual standard deviation $\sim 25\%$, $n=3$) due
275 to poorly repeatable migration times. At pH 4, near the isoelectric point of these
276 phages (Michen and Graule, 2010), the electrophoretic mobility of virions and the
277 EOF mobility should tend to zero. This results in a very slow migration of both virions
278 and DMSO (Fig. S2), which is detrimental to their separation and impairs the
279 measurement of migration times required to calculate the electrophoretic mobility of
280 virions.

281 The low precision in measurements at pH 11 is more difficult to explain and
282 should be the subject of further study. It can be hypothesized that increasing pH
283 values reduces the positive charges of protein domains near the RNA-coat protein
284 interface, thus destabilizing viral particle assembly. Moreover, the more alkaline the
285 media the more RNA spontaneously hydrolyses (Bock, 1967). This pH sensitivity has
286 even been exploited to 'empty' MS2 virions of their RNA (Hooker et al., 2004). Since
287 the electrokinetic properties of phages can, in some cases, be affected by the internal
288 RNA of virions (Dika et al., 2011; Langlet et al., 2008b), RNA spontaneous hydrolysis
289 at high pH may be responsible for the lack of precision at pH 11.

290 An optimal pH range was thus delimited from 5 to 10 at which the peaks of
291 phages and DMSO were well resolved with repeatable migration times, allowing an
292 accurate determination of $\mu_{native}^{phage, pH}$ (RSD lower than 5%, $n=3$). MS2, GA and Q β are
293 characterized by negative $\mu_{native}^{phage, pH}$ values that decreases with rising pH, clearly
294 showing the dynamic of the charge density of virions as a function of pH (Fig. 1b).

295 MS2 virions are more anionic than GA and Q β virions at all pH levels examined as
296 indicated by the low $\mu_{native}^{MS2, pH}$ values (Fig. 1b, red) in comparison with $\mu_{native}^{GA, pH}$ and
297 $\mu_{native}^{Q\beta, pH}$ values (Fig. 1b, green and blue, respectively).

298

299 **3.2. CZE assays with SDS-containing BGEs: SDS-modified electrophoretic** 300 **mobilities**

301 When performing CZE analyses in the presence of 10 mM SDS, the migration
302 order of MS2, Q β and GA phages was reversed, as compared to SDS-free
303 conditions. Indeed, while Q β and GA migrated faster than MS2 without SDS at pH 7
304 (Fig. 1a), they are slower than MS2 in SDS-containing BGE (Fig. 2a). Quantitatively,
305 the electrophoretic mobility of MS2 virions only decreased from $-3.09 \times 10^{-8} \text{ m}^2 \cdot \text{V}^{-1} \cdot \text{s}^{-1}$
306 without SDS to $-3.23 \times 10^{-8} \text{ m}^2 \cdot \text{V}^{-1} \cdot \text{s}^{-1}$ with SDS (20% decrease) indicating low
307 interactions between SDS molecules and MS2 virions. In contrast, the electrophoretic
308 mobility of Q β and GA virions decreased significantly, from $-1.35 \times 10^{-8} \text{ m}^2 \cdot \text{V}^{-1} \cdot \text{s}^{-1}$ to -
309 $3.66 \times 10^{-8} \text{ m}^2 \cdot \text{V}^{-1} \cdot \text{s}^{-1}$ for Q β (177% decrease) and from $-0.48 \times 10^{-8} \text{ m}^2 \cdot \text{V}^{-1} \cdot \text{s}^{-1}$ to -
310 $3.79 \times 10^{-8} \text{ m}^2 \cdot \text{V}^{-1} \cdot \text{s}^{-1}$ for GA (301% decrease). This indicates that SDS strongly
311 interact with GA and much less with Q β virions. Furthermore, since the larger the
312 SDS-induced electrophoretic mobility decrease, the more hydrophobic the virions
313 (Sautrey et al., 2018), these results suggest the hydrophobicity sequence
314 GA>Q β >MS2 consistently with earlier reports (Armanious et al., 2016; Dika et al.,
315 2013b).

316 The SDS-modified electrophoretic mobility ($\mu_{SDS-modified}^{phage, pH}$) of MS2, Q β and GA was
317 plotted against pH (Fig. 2b). Note that $\mu_{SDS-modified}^{GA, pH}$ and $\mu_{SDS-modified}^{Q\beta, pH}$ values are lower
318 than $\mu_{SDS-modified}^{MS2, pH}$ regardless of pH, except for Q β at pH 5, indicating higher negative

319 surface charge densities for GA and Q β than for MS2 virion in the presence of SDS.
 320 The $\mu_{SDS-modified}^{phage, pH}$ values variation against pH is irregular for each phage and interesting
 321 features can be observed. First, the $\mu_{SDS-modified}^{MS2, pH}$ and $\mu_{SDS-modified}^{GA, pH}$ values decrease
 322 almost linearly and similarly from pH 5 to 7 (Fig. 2b, red and green, respectively),
 323 while the $\mu_{SDS-modified}^{Q\beta, pH}$ value also decreases from pH 5 to 8 but more sharply (Fig. 2b,
 324 blue). Second, the $\mu_{SDS-modified}^{MS2, pH}$ value remains fairly stable from pH 7 to 10 (Fig. 2b,
 325 red), while the $\mu_{SDS-modified}^{GA, pH}$ and $\mu_{SDS-modified}^{Q\beta, pH}$ values suddenly increase at pH 8 and 9
 326 respectively, and then decrease again until pH 10 (Fig. 2b, green and blue,
 327 respectively). Overall, these data highlight that virion hydrophobicity varies non-
 328 linearly with pH, but this dynamic is different for each phage.

329

330 **3.3. SDS-free versus SDS-containing analyses: Phage hydrophobic index**

331 The $\mu_{SDS-modified}^{phage, pH}$ values alone are not sufficient to assess the hydrophobicity of
 332 virions because their surface charge density in the presence of SDS is obviously
 333 related to both the ionizable residues of the proteinaceous capsid and to the SDS
 334 molecules bound to the capsid. The native ionization of virions must thus be
 335 extracted from their SDS-modified charge density to quantify their hydrophobicity.
 336 The 'hydrophobic index' of phages depending on pH (H_{pH}^{phage}) can be calculated by
 337 subtracting the $\mu_{native}^{phage, pH}$ values from the associated $\mu_{SDS-modified}^{phage, pH}$ values, and used to
 338 describe the hydrophobicity of phages. Both mobilities should be expressed in terms
 339 of reduced mobilities (Radko et al., 2000), to result in dimensionless H_{pH}^{phage} values
 340 that can be easily compared between any non-enveloped virions (see Section 2.4).
 341 Following this definition, H_{pH}^{phage} values start from 0 and increase with hydrophobicity.

342 As shown in Fig. 3a, H_7^{MS2} is 0.10 ± 0.11 suggesting a very low hydrophobicity of MS2
343 virions at pH 7. In contrast, H_7^{QB} and H_7^{GA} are 1.73 ± 0.14 and 2.48 ± 0.13 , respectively.
344 These results modify the previously suggested hydrophobic sequence (Armanious et
345 al., 2016; Dika et al., 2013b) to GA>Qβ>>MS2.

346 The very low value of H_7^{MS2} is intriguing in comparison to the higher H_7^{GA} value.
347 Indeed, the MS2 and GA phages are very close in the evolutionary tree (Bollback
348 and Huelsenbeck, 2001) and in their structures (Pumpens et al., 2016). Based on
349 this reasoning, the theoretical hydrophobicity of the two capsid proteins of MS2 and
350 GA phages was determined from their primary sequences (Fig. 4). Notably, the first
351 60 amino acids (of ~130 for both phages) are rather hydrophilic, while the C-terminal
352 70 amino acids are rather hydrophobic. Interestingly, the hydrophobic residues are
353 present in longer stretches in the GA capsid protein (Fig. 4, solid line) than in MS2
354 (Fig. 4, dotted line). We thus suggest that the hydrophobic domains on the surface of
355 MS2 virions may be too small to allow the binding of the relatively bulky SDS
356 molecules, especially if they form micellar aggregates or other supramolecular
357 assemblies (Sautrey et al., 2018). Future investigations could focus on testing other
358 amphiphilic probes to increase the sensitivity of this method. Nevertheless, the
359 theoretical hydrophobicity of a virion deduced from the primary sequence of its capsid
360 protein is not correlated with that experimentally observed (Heldt et al., 2017),
361 possibly because the internal RNA and the RNA-capsid protein interface may affect
362 the physicochemical surface properties of virions (Dika et al., 2011; Langlet et al.,
363 2008b).

364 The hydrophobic index of phages (H_{pH}^{phage}) was also determined from pH 5 to 10
365 (Fig. 3b). Interestingly, the H_{pH}^{phage} values are fairly stable for all three phages but only
366 outside of a narrow pivotal pH range where values change suddenly. As shown in

367 Fig. 3b (green), H_{pH}^{GA} decreases slightly from pH 5 to 7 (5% per pH unit) and from pH
368 8 to 10 (8% per pH unit), while a sharp decrease occurs between pH 7 and 8 (26%
369 decrease). Similarly, $H_{pH}^{Q\beta}$ (Fig. 3b, blue) is almost unchanged from pH 5 to 8 and
370 from 9 to 10 (<3% per pH unit), whereas a sharp drop occurs between pH 8 and 9
371 (31% decrease). Lastly, H_{pH}^{MS2} (Fig. 3b, red) drops from pH 5 to 6 (68%) but is then
372 stable from pH 6 to 10. These data indicate a pivotal pH at which the hydrophobicity
373 of virions decreases sharply and which is specific for each phage. This has not been
374 observed using other methodologies or other non-enveloped viruses, and may be
375 indicative of a structural rearrangement of virions in response to pH changes that
376 affects hydrophobic domains on the capsid (Roshal et al., 2019; Song et al., 2020).
377 Note that the pivotal pH values of hydrophobicity do not match the isoelectric point of
378 these phages, which is below pH 4 (Michen and Graule, 2010), and that the curves of
379 H_{pH}^{GA} and $H_{pH}^{Q\beta}$ versus pH do not overlap with the corresponding curves of native
380 electrophoretic mobility (Fig. 5, middle and right panels). This supports the idea that
381 the hydrophobicity dynamics of virions is not solely related to the ionization of the
382 capsid, especially since other constituents, notably internal RNA, play a role in their
383 structuring (Koning et al., 2016). Conversely, the H_{pH}^{MS2} versus pH curve overlaps the
384 corresponding curve of native electrophoretic mobility (Fig. 5, left panel). This could
385 be due to the low hydrophobicity of MS2 virions, at any pH, in comparison with Q β
386 and GA (Fig. 3a and 3b). Our observation of a pivotal pH of virion hydrophobicity
387 requires further study to explain the phenomenon at a molecular level.

388 The finding of the pivotal pH of hydrophobicity means that minor pH variations
389 may have a strong impact on the adhesion of virions onto surfaces, and therefore on
390 their dissemination in both the environment and living organisms. For example,

391 enteric virions have been shown to accumulate on riverbed sediments where they
392 can be “stored” and released later to infect a new host (Bosch et al., 2006; Rao et al.,
393 1986). These adsorption/desorption processes depend on both the electrical charge
394 and hydrophobicity of virions (Fauvel et al., 2019), both varying with pH as we have
395 shown here for hydrophobicity. Moreover, the change in hydrophobicity of GA and
396 MS2 at different pH values may help explain discrepancies in their behavior at
397 interfaces when comparing the removal efficiency of virions from aqueous media
398 ranging from pH 7.6 to 8.2 (Boudaud et al., 2012) versus their adhesion on
399 hydrophobic surfaces under controlled pH conditions (Dika et al., 2013b). This clearly
400 shows that further understanding how virion hydrophobicity varies, including pH but
401 also other factors e.g., temperature (Brié et al., 2016), is essential to improve the
402 process of water decontamination. Enteric virus pollution in water remains a major
403 cause of viral outbreaks responsible for millions of infections in humans every year
404 (Upfold et al., 2021). Note that the pH variation in virion hydrophobicity also may
405 impact non-specific interactions with all kinds of biological components *in vivo*,
406 especially if the virions pivotal pH of hydrophobicity is in a physiological pH range.
407 For example, the entrapment of in-blood phages by the reticuloendothelial system
408 may need to be controlled to ensure success during phage therapy (Merril et al.,
409 1996). The persistence of virions in blood is indeed variable even for closely related
410 phages (Serwer et al., 2021), just as we observed a marked difference in the
411 hydrophobicity features of MS2 and GA phages. The measurement of virion
412 hydrophobicity and the determination of a pivotal pH should thus be integrated into
413 the framework of future studies dealing with the survival of phages in blood, their
414 infectivity and their pathogenicity, and more generally with their dissemination in the
415 human body.

416 **4. Conclusion**

417 The hydrophobicity of three non-enveloped virions was quantified here as a
418 function of pH by using SDS to label capsid hydrophobic domains and CZE as
419 sensing technique. This relatively simple and fast procedure can be applied under
420 various physicochemical conditions in order to identify factors affecting virion
421 hydrophobicity. The hydrophobic index defined here could be adopted as a standard
422 parameter in describing the hydrophobicity of non-enveloped viruses. The virion
423 hydrophobicity changes at a virion-specific pivotal pH require further investigation as
424 its existence may reflect unknown structural dynamics of virions and could have
425 broad implications in their pathogenicity and dissemination. This report concerns only
426 non-enveloped +ssRNA icosahedral viruses but the approach developed can also be
427 applied to other and diverse virus families of significance to human health and the
428 environment.

429

430 **Appendix A**

431 The BGEs used in this study were prepared to keep a constant ionic strength (10
432 mM) regardless of pH. The total phosphate concentration as well as the
433 corresponding volume of 0.85% H₃PO₄ aqueous stock solution (146 mM) required for
434 200 mL of BGE are reported in Table A1 as a function of pH. Briefly, the required
435 volume of 0.85% H₃PO₄ was taken, 150 mL pure water was added and the pH was
436 adjusted with 1 M NaOH; the final volume was adjusted with pure water.

437 **Table A1.** Total phosphate concentration and corresponding volume of 0.85%
438 H₃PO₄ aqueous solution (146 mM) required for the preparation of 200 mL of 10 mM
439 ionic strength BGEs.

pH	Total phosphate concentration (mM)	Volume of H ₃ PO ₄ 0,85% (mL)
4	10.13	13.86
5	9.88	13.52
6	9.62	13.16
7	8.94	12.23
8	7.50	10.26
9	5.64	7.72
10	4.29	5.87
11	3.67	5.02

440

441

442 **Acknowledgement**

443 We gratefully acknowledge Pr R. Duval, faculty director of Faculté de Pharmacie
444 de Nancy (Université de Lorraine, Nancy, France), for access to the capillary
445 electrophoresis instrument and Pr. I. Clarot (EA 3452 CITHEFOR, Université de
446 Lorraine, Nancy, France) for valuable discussions. We thank also J. Challant (UMR
447 7564 LCPME, CNRS-Université de Lorraine, Nancy, France) for assistance in
448 phages production and purification as well as the colleagues of the laboratory for the
449 English revision of the manuscript. Finally, we acknowledge the anonymous
450 Reviewers as well as Ian J. Molineux (Editor) for their much-appreciated contributions
451 in improving this paper.

452

453 **CRedit authors contribution statement**

454 **Guillaume Bastin:** Conceptualization, Resources, Formal analysis, Writing –
455 Original Draft, Visualization. **Christophe Gantzer:** Conceptualization, Writing –
456 Review & Editing. **Guillaume Sautrey:** Conceptualization, Methodology, Validation,
457 Formal analysis, Investigation, Resources, Writing – Original Draft, Writing – Review
458 & Editing, Visualization, Supervision, Project administration.

459

460 **Declaration of competing interest**

461 The authors have no conflicts of interest.

462

463 **Funding**

464 This work was supported by French Ministry of Higher Education and Research
465 and the French National Scientific Research Center (CNRS), as well as the
466 University of Lorraine. This research received no external funding.

467 **References**

- 468 Armanious, A., Aeppli, M., Jacak, R., Refardt, D., Sigstam, T., Kohn, T., Sander, M.,
469 2016. Viruses at Solid-Water Interfaces: A Systematic Assessment of
470 Interactions Driving Adsorption. *Environ. Sci. Technol.* 50, 732–743.
471 <https://doi.org/10.1021/acs.est.5b04644>
- 472 Bastin, G., Loison, P., Vernex-Loiset, L., Dupire, F., Challant, J., Majou, D., Boudaud,
473 N., Krier, G., Gantzer, C., 2020. Structural Organizations of Q β and MS2 Phages
474 Affect Capsid Protein Modifications by Oxidants Hypochlorous Acid and
475 Peroxynitrite. *Front. Microbiol.* 11, 1–13.
476 <https://doi.org/10.3389/fmicb.2020.01157>
- 477 Bock, R.M., 1967. [29] Alkaline hydrolysis of RNA. *Methods Enzymol.* 12, 224–228.
478 [https://doi.org/10.1016/s0076-6879\(67\)12035-1](https://doi.org/10.1016/s0076-6879(67)12035-1)
- 479 Bollback, J.P., Huelsenbeck, J.P., 2001. Phylogeny, genome evolution, and host
480 specificity of single-stranded RNA bacteriophage (family Leviviridae). *J. Mol.*
481 *Evol.* 52, 117–128. <https://doi.org/10.1007/s002390010140>
- 482 Bosch, A., Pintó, R.M., Abad, F.X., 2006. Survival and Transport of Enteric Viruses in
483 the Environment, in: Goyal, S.M. (Ed.), *Viruses in Foods*. Springer US, Boston,
484 MA, pp. 151–187. https://doi.org/10.1007/0-387-29251-9_6
- 485 Boudaud, N., Machinal, C., David, F., Fréval-Le Bourdonnec, A., Jossent, J.,
486 Bakanga, F., Arnal, C., Jaffrezic, M.P., Oberti, S., Gantzer, C., 2012. Removal of
487 MS2, Q β and GA bacteriophages during drinking water treatment at pilot scale.
488 *Water Res.* 46, 2651–2664. <https://doi.org/10.1016/j.watres.2012.02.020>
- 489 Brié, A., Bertrand, I., Meo, M., Boudaud, N., Gantzer, C., 2016. The Effect of Heat on
490 the Physicochemical Properties of Bacteriophage MS2. *Food Environ. Virol.* 8,
491 251–261. <https://doi.org/10.1007/s12560-016-9248-2>
- 492 Cui, Z., Gorzelnik, K. V., Chang, J.Y., Langlais, C., Jakana, J., Young, R., Zhang, J.,
493 2017. Structures of Q β virions, virus-like particles, and the Q β –MurA complex
494 reveal internal coat proteins and the mechanism of host lysis. *Proc. Natl. Acad.*
495 *Sci. U. S. A.* 114, 11697–11702. <https://doi.org/10.1073/pnas.1707102114>
- 496 Dent, K.C., Thompson, R., Barker, A.M., Hiscox, J.A., Barr, J.N., Stockley, P.G.,
497 Ranson, N.A., 2013. The asymmetric structure of an icosahedral virus bound to
498 its receptor suggests a mechanism for genome release. *Structure* 21, 1225–
499 1234. <https://doi.org/10.1016/j.str.2013.05.012>
- 500 Dika, C., Duval, J.F.L., Francius, G., Perrin, A., Gantzer, C., 2015. Isoelectric point is
501 an inadequate descriptor of MS2, Phi X 174 and PRD1 phages adhesion on
502 abiotic surfaces. *J. Colloid Interface Sci.* 446, 327–334.
503 <https://doi.org/10.1016/j.jcis.2014.08.055>
- 504 Dika, C., Duval, J.F.L., Ly-Chatain, H.M., Merlin, C., Gantzer, C., 2011. Impact of
505 internal RNA on aggregation and electrokinetics of viruses: comparison between
506 MS2 phage and corresponding virus-like particles. *Appl. Environ. Microbiol.* 77,
507 4939–48. <https://doi.org/10.1128/AEM.00407-11>

508 Dika, C., Gantzer, C., Perrin, A., Duval, J.F.L., 2013a. Impact of the virus purification
509 protocol on aggregation and electrokinetics of MS2 phages and corresponding
510 virus-like particles. *Phys. Chem. Chem. Phys.* 15, 5691–5700.
511 <https://doi.org/10.1039/c3cp44128h>

512 Dika, C., Ly-Chatain, M.H., Francius, G., Duval, J.F.L., Gantzer, C., 2013b. Non-
513 DLVO adhesion of F-specific RNA bacteriophages to abiotic surfaces:
514 Importance of surface roughness, hydrophobic and electrostatic interactions.
515 *Colloids Surfaces A Physicochem. Eng. Asp.* 435, 178–187.
516 <https://doi.org/10.1016/j.colsurfa.2013.02.045>

517 Farkas, K., Walker, D.I., Adriaenssens, E.M., McDonald, J.E., Hillary, L.S., Malham,
518 S.K., Jones, D.L., 2020. Viral indicators for tracking domestic wastewater
519 contamination in the aquatic environment. *Water Res.* 181, 115926.
520 <https://doi.org/10.1016/j.watres.2020.115926>

521 Fauvel, B., Cauchie, H.M., Gantzer, C., Ogorzaly, L., 2019. Influence of physico-
522 chemical characteristics of sediment on the in situ spatial distribution of F-
523 specific RNA phages in the riverbed. *FEMS Microbiol. Ecol.* 95, 1–11.
524 <https://doi.org/10.1093/femsec/fiy240>

525 Gerba, C.P., 1984. Applied and Theoretical Aspects of Virus Adsorption to Surfaces.
526 *Adv. Appl. Microbiol.* 30, 133–168. [https://doi.org/10.1016/S0065-](https://doi.org/10.1016/S0065-2164(08)70054-6)
527 [2164\(08\)70054-6](https://doi.org/10.1016/S0065-2164(08)70054-6)

528 Golmohammadi, R., Fridborg, K., Bundule, M., Valegård, K., Liljas, L., 1996. The
529 crystal structure of bacteriophage Q β at 3.5 Å resolution. *Structure* 4, 543–554.
530 [https://doi.org/10.1016/S0969-2126\(96\)00060-3](https://doi.org/10.1016/S0969-2126(96)00060-3)

531 Golmohammadi, R., Valegård, K., Fridborg, K., Liljas, L., 1993. The Refined Structure
532 of Bacteriophage MS2 at 2.8 Å Resolution. *J. Mol. Biol.*
533 <https://doi.org/10.1006/jmbi.1993.1616>

534 Heffron, J., Mayer, B.K., 2021. Virus Isoelectric Point Estimation: Theories and
535 Methods. *Appl. Environ. Microbiol.* 87, 1–17. [https://doi.org/10.1128/AEM.02319-](https://doi.org/10.1128/AEM.02319-20)
536 [20](https://doi.org/10.1128/AEM.02319-20)

537 Heldt, C.L., Zahid, A., Vijayaragavan, K.S., Mi, X., 2017. Experimental and
538 computational surface hydrophobicity analysis of a non-enveloped virus and
539 proteins. *Colloids Surfaces B Biointerfaces* 153, 77–84.
540 <https://doi.org/10.1016/j.colsurfb.2017.02.011>

541 Hodgson, K.R., Torok, V.A., Turnbull, A.R., 2017. Bacteriophages as enteric viral
542 indicators in bivalve mollusc management. *Food Microbiol.* 65, 284–293.
543 <https://doi.org/10.1016/j.fm.2017.03.003>

544 Hooker, J.M., Kovacs, E.W., Francis, M.B., 2004. Interior Surface Modification of
545 Bacteriophage MS2. *J. Am. Chem. Soc.* 126, 3718–3719.
546 <https://doi.org/10.1021/ja031790q>

547 Hunter, R.J., 1981a. Chapter 2 - Charge and Potential Distribution at Interfaces, in:
548 HUNTER, R.J. (Ed.), *Zeta Potential in Colloid Science*. Academic Press, pp. 11–
549 58. <https://doi.org/https://doi.org/10.1016/B978-0-12-361961-7.50006-7>

550 Hunter, R.J., 1981b. Chapter 3 - The Calculation of Zeta Potential, in: HUNTER, R.J.
551 (Ed.), *Zeta Potential in Colloid Science*. Academic Press, pp. 59–124.
552 <https://doi.org/https://doi.org/10.1016/B978-0-12-361961-7.50007-9>

553 Joonaki, E., Hassanpouryouzband, A., Heldt, C.L., Areo, O., 2020. Surface
554 Chemistry Can Unlock Drivers of Surface Stability of SARS-CoV-2 in a Variety of
555 Environmental Conditions. *Chem* 6, 2135–2146.
556 <https://doi.org/10.1016/j.chempr.2020.08.001>

557 Kenndler, E., 2001. Capillary electrophoresis of macromolecular biological
558 assemblies : bacteria and viruses 20, 543–551.

559 Koning, R.I., Gomez-Blanco, J., Akopjana, I., Vargas, J., Kazaks, A., Tars, K.,
560 Carazo, J.M., Koster, A.J., 2016. Asymmetric cryo-EM reconstruction of phage
561 MS2 reveals genome structure in situ. *Nat. Commun.* 7, 1–6.
562 <https://doi.org/10.1038/ncomms12524>

563 Kuhn, R., Hoffstetter-Kuhn, S., 1993. *Capillary Electrophoresis: Principles and*
564 *Practice*. Springer-Verlag, Berlin. <https://doi.org/10.1007/978-3-642-78058-5>

565 Langlet, J., Gaboriaud, F., Duval, J.F.L., Gantzer, C., 2008a. Aggregation and
566 surface properties of F-specific RNA phages: Implication for membrane filtration
567 processes. *Water Res.* 42, 2769–2777.
568 <https://doi.org/10.1016/j.watres.2008.02.007>

569 Langlet, J., Gaboriaud, F., Gantzer, C., Duval, J.F.L., 2008b. Impact of chemical and
570 structural anisotropy on the electrophoretic mobility of spherical soft multilayer
571 particles: the case of bacteriophage MS2. *Biophys. J.* 94, 3293–3312.
572 <https://doi.org/10.1529/biophysj.107.115477>

573 Merril, C.R., Biswas, B., Carlton, R., Jensen, N.C., Creed, G.J., Zullo, S., Adhya, S.,
574 1996. Long-circulating bacteriophage as antibacterial agents. *Proc. Natl. Acad.*
575 *Sci. U. S. A.* 93, 3188–3192. <https://doi.org/10.1073/pnas.93.8.3188>

576 Michen, B., Graule, T., 2010. Isoelectric points of viruses. *J. Appl. Microbiol.* 109,
577 388–397. <https://doi.org/10.1111/j.1365-2672.2010.04663.x>

578 Pumpens, P., Renhofa, R., Dishlers, A., Kozlovskas, T., Ose, V., Pushko, P., Tars, K.,
579 Grens, E., Bachmann, M.F., 2016. The true story and advantages of RNA phage
580 capsids as nanotools. *Intervirology* 59, 74–100.
581 <https://doi.org/10.1159/000449503>

582 Radko, S.P., Stastna, M., Chrambach, A., 2000. Size-Dependent Electrophoretic
583 Migration and Separation of Liposomes by Capillary Zone Electrophoresis in
584 Electrolyte Solutions of Various Ionic Strengths 72, 5955–5960.

585 Rao, V.C., Metcalf, T.G., Melnick, J.L., 1986. Human viruses in sediments, sludges,
586 and soils. *Bull. World Health Organ.* 64, 1–14.
587 <https://doi.org/10.1201/9780429270475>

588 Roshal, D., Konevtsova, O., Božič, A.L., Podgornik, R., Rochal, S., 2019. pH-induced
589 morphological changes of proteinaceous viral shells 1–9.
590 <https://doi.org/10.1038/s41598-019-41799-6>

591 Sautrey, G., Brié, A., Gantzer, C., Walcarius, A., 2018. MS2 and Q β bacteriophages
592 reveal the contribution of surface hydrophobicity on the mobility of non-
593 enveloped icosahedral viruses in SDS-based capillary zone electrophoresis.
594 *Electrophoresis* 39, 377–385. <https://doi.org/10.1002/elps.201700352>

595 Serwer, P., Wright, E.T., De La Chapa, J., Gonzales, C.B., 2021. Basics for improved
596 use of phages for therapy. *Antibiotics* 10, 1–12.
597 <https://doi.org/10.3390/antibiotics10060723>

598 Shi, H., Tarabara, V. V., 2018. Charge, size distribution and hydrophobicity of
599 viruses: Effect of propagation and purification methods. *J. Virol. Methods* 256,
600 123–132. <https://doi.org/10.1016/j.jviromet.2018.02.008>

601 Shintani, H., 1997. *Handbook of Capillary Electrophoresis Applications*. Springer,
602 Dordrecht. <https://doi.org/https://doi.org/10.1007/978-94-009-1561-9>

603 Shirasaki, N., Matsushita, T., Matsui, Y., Urasaki, T., Ohno, K., 2009. Comparison of
604 behaviors of two surrogates for pathogenic waterborne viruses, bacteriophages
605 Q?? and MS2, during the aluminum coagulation process. *Water Res.* 43, 605–
606 612. <https://doi.org/10.1016/j.watres.2008.11.002>

607 Song, C., Takai-Todaka, R., Miki, M., Haga, K., Fujimoto, A., Ishiyama, R., Oikawa,
608 K., Yokoyama, M., Miyazaki, N., Iwasaki, K., Murakami, K., Katayama, K.,
609 Murata, K., 2020. Dynamic rotation of the protruding domain enhances the
610 infectivity of norovirus. *PLoS Pathog.* 16, 1–24.
611 <https://doi.org/10.1371/journal.ppat.1008619>

612 Stefan, M.I., Le Novère, N., 2013. Cooperative Binding. *PLoS Comput. Biol.* 9, 2–7.
613 <https://doi.org/10.1371/journal.pcbi.1003106>

614 Tars, K., Bundule, M., Fridborg, K., Liljas, L., 1997. The crystal structure of
615 bacteriophage GA and a comparison of bacteriophages belonging to the major
616 groups of *Escherichia coli* leviviruses. *J. Mol. Biol.* 271, 759–773.

617 Upfold, N.S., Luke, G.A., Knox, C., 2021. Occurrence of Human Enteric Viruses in
618 Water Sources and Shellfish: A Focus on Africa, Food and Environmental
619 Virology. Springer US. <https://doi.org/10.1007/s12560-020-09456-8>

620

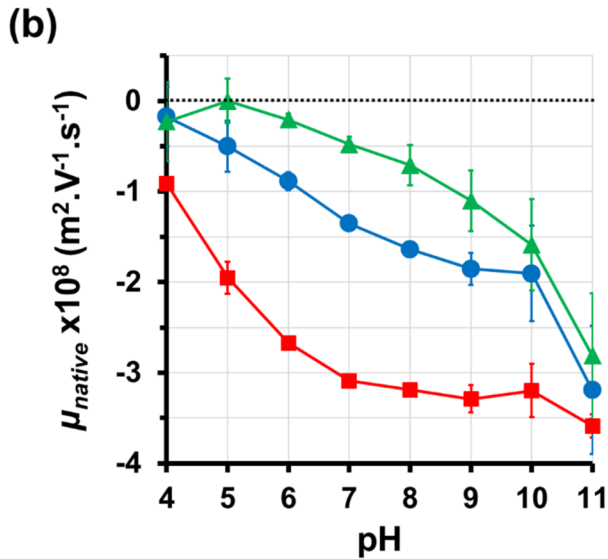
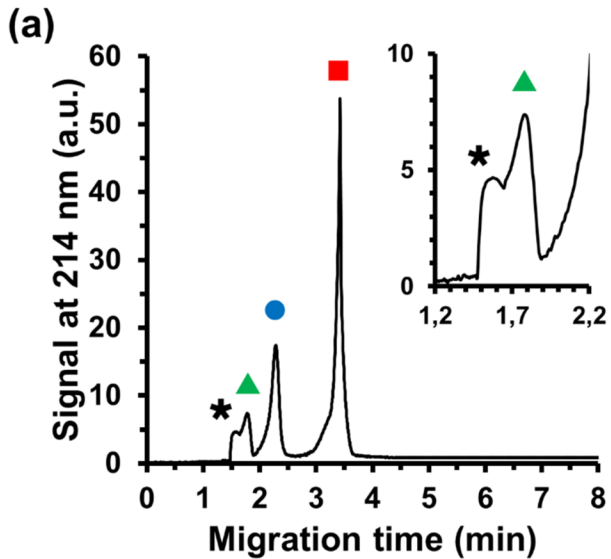
1 **Fig. 1.** Electrokinetic properties of phages in SDS-free CZE. **(a)** Representative
2 electropherogram obtained at pH 7 with a pooled sample of MS2 (■), Qβ (●) and GA
3 (▲) co-injected with a 0.005% v/v DMSO aqueous solution (✱). The inset is an
4 enlargement near the peaks of DMSO (✱) and GA (▲). BGE: 8.94 mM phosphoric
5 acid adjusted to pH 7.0 (10 mM ionic strength). **(b)** pH-dependent variations in the
6 native electrophoretic mobility $\mu_{native}^{phage, pH}$ of MS2 (■), Qβ (●) and GA (▲) measured by
7 means of CZE analyses performed with different BGEs ranging from pH 4 to 11 (all 10
8 mM ionic strength). The dotted line indicates the isoelectric point ($\mu_{native}^{phage, pH} = 0$). Error
9 bars are standard deviation (n=3).

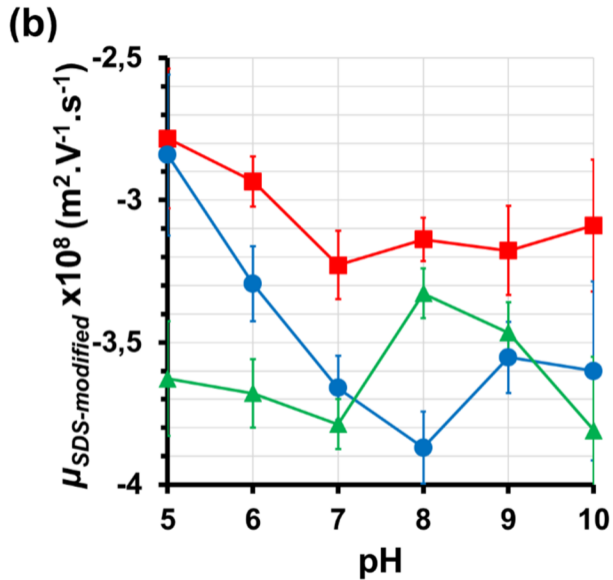
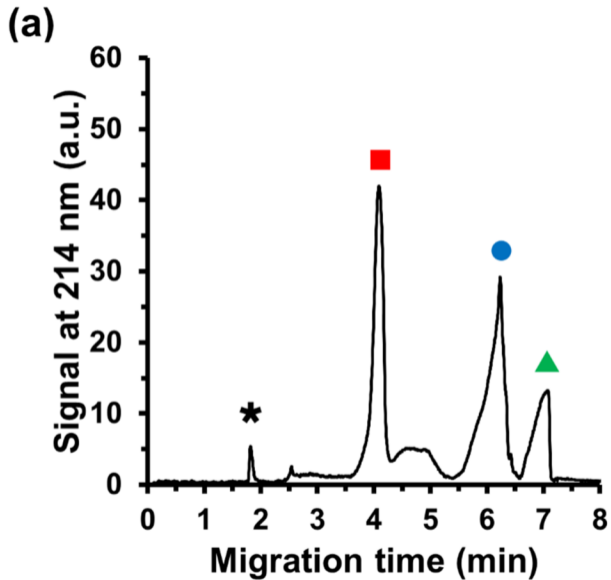
1 **Fig. 2.** Electrokinetic properties of phages in SDS-containing CZE. (a) Representative
2 electropherogram obtained at pH 7 with a pooled sample of MS2 (■), Qβ (●) and GA
3 (▲) co-injected with a 0.005% v/v DMSO aqueous solution (✱). BGE: 8.94 mM
4 phosphoric acid adjusted to pH 7.0 (10 mM ionic strength) supplemented with 10 mM
5 SDS. (b) pH-dependent variations in the SDS-modified electrophoretic mobility
6 $\mu_{SDS-modified}^{phage, pH}$ of MS2 (■), Qβ (●) and GA (▲) obtained as for Figure 1, but in the
7 presence of 10 mM SDS. Error bars are standard deviation (n=3).

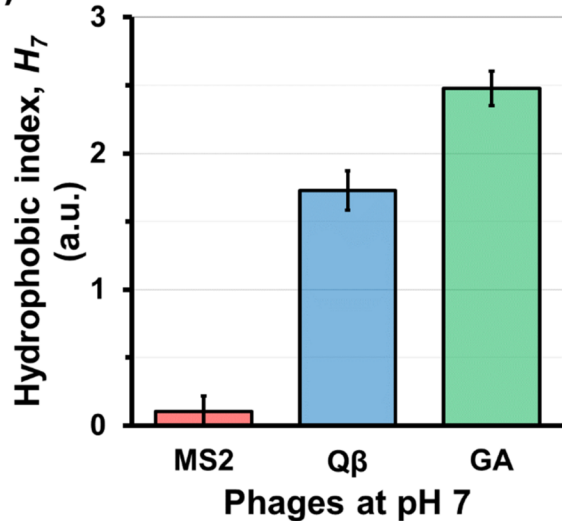
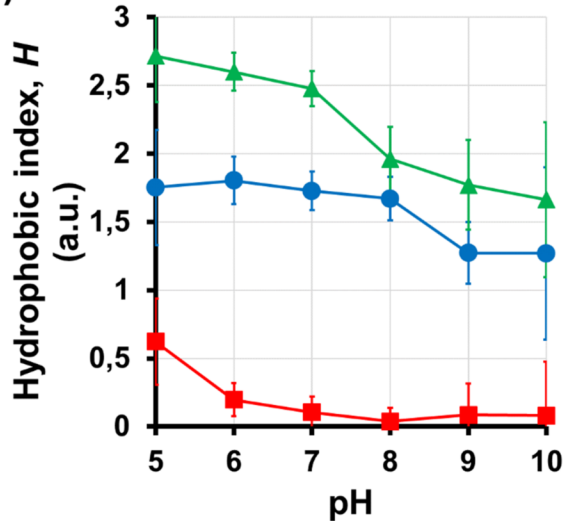
1 **Fig. 3.** Assessment of phages hydrophobicity as a function of pH. **(a)** comparison of
2 the hydrophobic indexes found at pH 7 for MS2 (red), Q β (blue) and GA (green). **(b)**
3 pH-dependent variations in the hydrophobic index of MS2 (■), Q β (●) and GA (▲).
4 Error bars are the sum of standard deviations related to the electrophoretic mobilities
5 of native and SDS-modified phages.

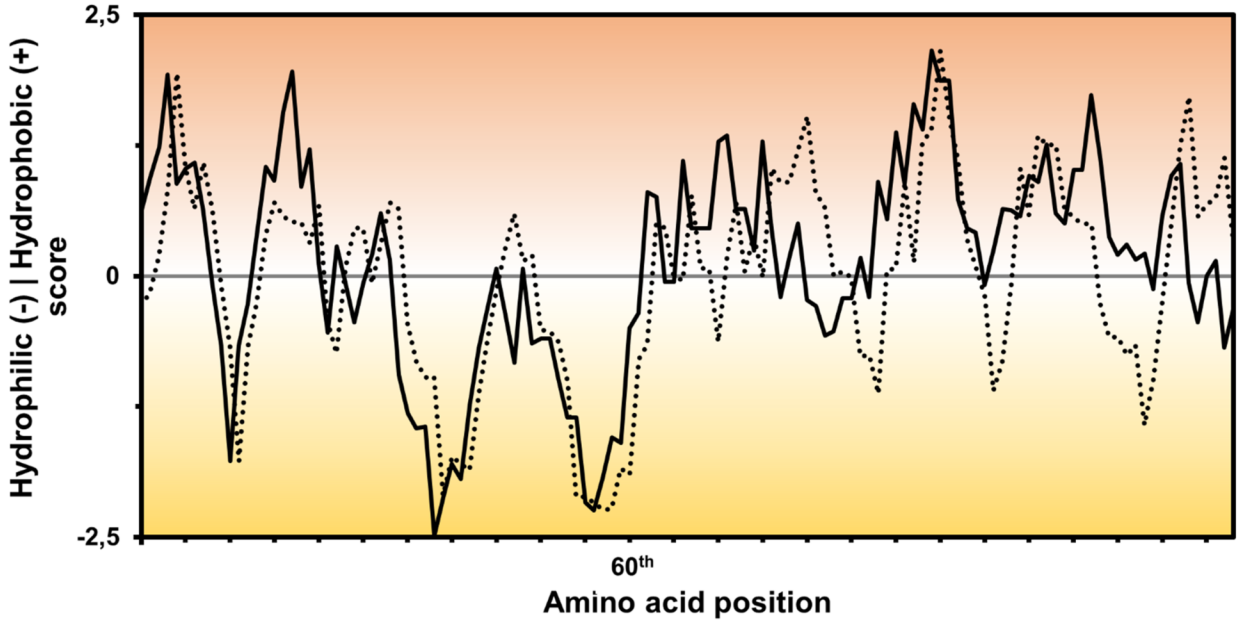
1 **Fig. 4.** Hydrophilic/hydrophobic balance for capsid protein of GA and MS2 phages.
2 Hydrophobic amino acids provide positive score (+) while the hydrophilic ones provide
3 negative score (-). Dotted line: MS2. Solid line: GA. Results obtained from the online
4 'protscale' software using a 'Kyte and Doolittle' algorithm and a smoothing average
5 window through 7 amino acids. The primary sequences of capsid protein of GA and
6 MS2 used are from the database 'UniprotKB' under reference #P07234 and #P03612
7 for GA and MS2, respectively.

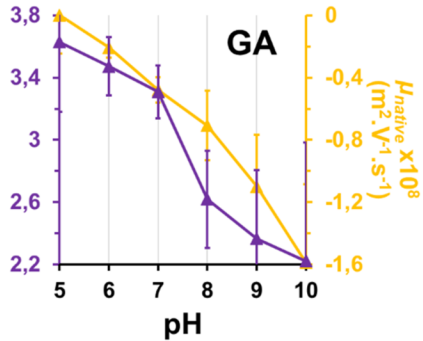
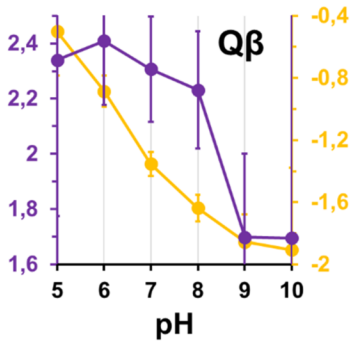
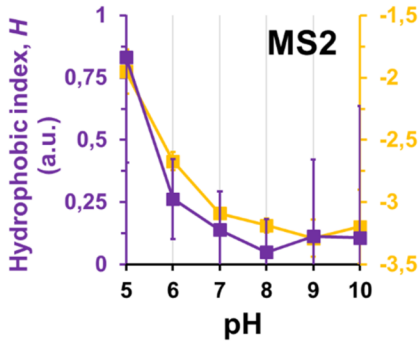
1 **Fig. 5.** Overlaps of phages hydrophobicity and native electrophoretic mobility as a
2 function of pH. Hydrophobic indexes H_{pH}^{phage} (left axis, purple) and native electrophoretic
3 mobilities $\mu_{native}^{phage, pH}$ (right axis, orange) of MS2 (left, ■), Q β (middle, ●) and GA (right,
4 ▲). Error bars are standard deviations (n=6 for hydrophobic index, n=3 for
5 electrophoretic mobility).



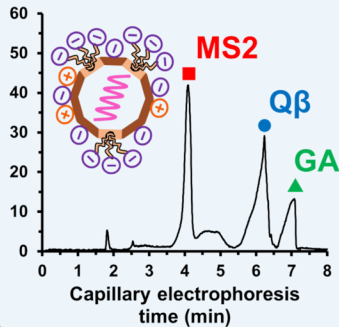


(a)**(b)**

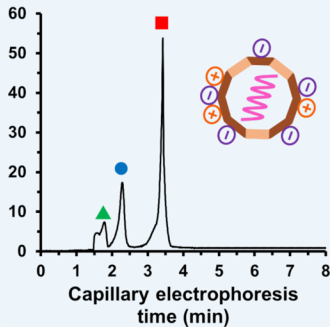




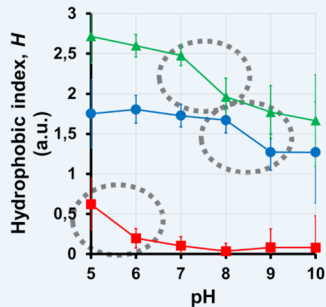
Virion in the presence of SDS



Virion in the absence of SDS




Virion hydrophobicity



 : Sodium dodecyl-sulfate (SDS)

 : Capsid hydrophobic domain

 : Virion hydrophobicity jump